JOURNAL OF Applied Polymer SCIENCE

Special Issue: Microfiltration and Ultrafiltration Membrane Science and Technology

Guest Editors: Prof. Isabel C. Escobar (University of Toledo) and Prof. Bart Van der Bruggen (University of Leuven)

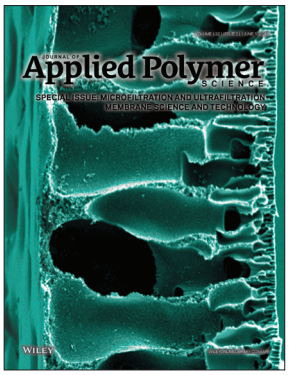

EDITORIAL

Microfiltration and Ultrafiltration Membrane Science and Technology
I. C. Escobar and B. Van der Bruggen, *J. Appl. Polym. Sci.* 2015, **DOI: 10.1002/app.42002**

REVIEWS

Nanoporous membranes generated from self-assembled block polymer precursors: *Quo Vadis*?
Y. Zhang, J. L. Sargent, B. W. Boudouris and W. A. Phillip, *J. Appl. Polym. Sci.* 2015, **DOI: 10.1002/app.41683**

Making polymeric membranes anti-fouling via "grafting from" polymerization of zwitterions
Q. Li, J. Imbrogno, G. Belfort and X.-L. Wang, *J. Appl. Polym. Sci.* 2015, **DOI: 10.1002/app.41781**

Fouling control on MF/ UF membranes: Effect of morphology, hydrophilicity and charge
R. Kumar and A. F. Ismail, *J. Appl. Polym. Sci.* 2015, **DOI: 10.1002/app.42042**

EMERGING MATERIALS AND FABRICATION

Preparation of a poly(phthalazine ether sulfone ketone) membrane with propanedioic acid as an additive and the prediction of its structure
P. Qin, A. Liu and C. Chen, *J. Appl. Polym. Sci.* 2015, **DOI: 10.1002/app.41621**

Preparation and characterization of MOF-PES ultrafiltration membranes
L. Zhai, G. Li, Y. Xu, M. Xiao, S. Wang and Y. Meng, *J. Appl. Polym. Sci.* 2015, **DOI: 10.1002/app.41663**

Tailoring of structures and permeation properties of asymmetric nanocomposite cellulose acetate/silver membranes
A. S. Figueiredo, M. G. Sánchez-Loredo, A. Maurício, M. F. C. Pereira, M. Minhalma and M. N. de Pinho, *J. Appl. Polym. Sci.* 2015, **DOI: 10.1002/app.41796**

LOW-FOULING POLYMERS

Low fouling polysulfone ultrafiltration membrane via click chemistry
Y. Xie, R. Tayouo and S. P. Nunes, *J. Appl. Polym. Sci.* 2015, **DOI: 10.1002/app.41549**

Elucidating membrane surface properties for preventing fouling of bioreactor membranes by surfactin
N. Behary, D. Lecouturier, A. Perwuelz and P. Dhulster, *J. Appl. Polym. Sci.* 2015, **DOI: 10.1002/app.41622**

PVC and PES-*g*-PEGMA blend membranes with improved ultrafiltration performance and fouling resistance
S. Jiang, J. Wang, J. Wu and Y. Chen, *J. Appl. Polym. Sci.* 2015, **DOI: 10.1002/app.41726**

Improved antifouling properties of TiO_2/PVDF nanocomposite membranes in UV coupled ultrafiltration
M. T. Moghadam, G. Lesage, T. Mohammadi, J.-P. Mericq, J. Mendret, M. Heran, C. Faur, S. Brosillon, M. Hemmati and F. Naeimpoor, *J. Appl. Polym. Sci.* 2015, **DOI: 10.1002/app.41731**

Development of functionalized doped carbon nanotube/polysulfone nanofiltration membranes for fouling control
P. Xie, Y. Li and J. Qiu, *J. Appl. Polym. Sci.* 2015, **DOI: 10.1002/app.41835**

JOURNAL OF Applied Polymer SCIENCE

Special Issue: Microfiltration and Ultrafiltration Membrane Science and Technology

Guest Editors: Prof. Isabel C. Escobar (University of Toledo) and
Prof. Bart Van der Bruggen (University of Leuven)

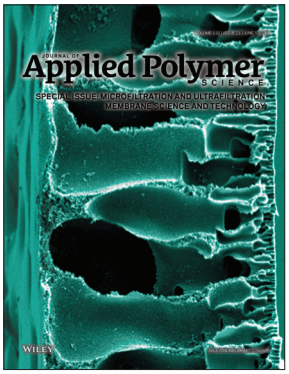

SURFACE MODIFICATION OF POLYMER MEMBRANES

Highly chlorine and oily fouling tolerant membrane surface modifications by *in situ* polymerization of dopamine and poly(ethylene glycol) diacrylate for water treatment
K. Yokwana, N. Gumbi, F. Adams, S. Mhlanga, E. Nxumalo and B. Mamba, *J. Appl. Polym. Sci.* 2015, **DOI: 10.1002/app.41661**

Fouling control through the hydrophilic surface modification of poly(vinylidene fluoride) membranes
H. Jang, D.-H. Song, I.-C. Kim, and Y.-N. Kwon, *J. Appl. Polym. Sci.* 2015, **DOI: 10.1002/app.41712**

Hydroxyl functionalized PVDF-TiO_2 ultrafiltration membrane and its antifouling properties
Y. H. Teow, A. A. Latif, J. K. Lim, H. P. Ngang, L. Y. Susan and B. S. Ooi, *J. Appl. Polym. Sci.* 2015, **DOI: 10.1002/app.41844**

Enhancing the antifouling properties of polysulfone ultrafiltration membranes by the grafting of poly(ethylene glycol) derivatives via surface amidation reactions
H. Yu, Y. Cao, G. Kang, Z. Liu, W. Kuang, J. Liu and M. Zhou, *J. Appl. Polym. Sci.* 2015, **DOI: 10.1002/app.41870**

SEPARATION APPLICATIONS

Experiment and simulation of the simultaneous removal of organic and inorganic contaminants by micellar enhanced ultrafiltration with mixed micelles
A. D. Vibhandik, S. Pawar and K. V. Marathe, *J. Appl. Polym. Sci.* 2015, **DOI: 10.1002/app.41435**

Polymeric membrane modification using SPEEK and bentonite for ultrafiltration of dairy wastewater
A. Pagidi, Y. Lukka Thuyavan, G. Arthanareeswaran, A. F. Ismail, J. Jaafar and D. Paul, *J. Appl. Polym. Sci.* 2015, **DOI: 10.1002/app.41651**

Forensic analysis of degraded polypropylene hollow fibers utilized in microfiltration
X. Lu, P. Shah, S. Maruf, S. Ortiz, T. Hoffard and J. Pellegrino, *J. Appl. Polym. Sci.* 2015, **DOI: 10.1002/app.41553**

A surface-renewal model for constant flux cross-flow microfiltration
S. Jiang and S. G. Chatterjee, *J. Appl. Polym. Sci.* 2015, **DOI: 10.1002/app.41778**

Ultrafiltration of aquatic humic substances through magnetically responsive polysulfone membranes
N. A. Azmi, Q. H. Ng and S. C. Low, *J. Appl. Polym. Sci.* 2015, **DOI: 10.1002/app.41874**

BIOSEPARATIONS APPLICATIONS

Analysis of the effects of electrostatic interactions on protein transport through zwitterionic ultrafiltration membranes using protein charge ladders
M. Hadidi and A. L. Zydney, *J. Appl. Polym. Sci.* 2015, **DOI: 10.1002/app.41540**

Modification of microfiltration membranes by hydrogel impregnation for pDNA purification
P. H. Castilho, T. R. Correia, M. T. Pessoa de Amorim, I. C. Escobar, J. A. Queiroz, I. J. Correia and A. M. Morão, *J. Appl. Polym. Sci.* 2015, **DOI: 10.1002/app.41610**

Hemodialysis membrane surface chemistry as a barrier to lipopolysaccharide transfer
B. Madsen, D. W. Britt, C.-H. Ho, M. Henrie, C. Ford, E. Stroup, B. Maltby, D. Olmstead and M. Andersen, *J. Appl. Polym. Sci.* 2015, **DOI: 10.1002/app.41550**

Membrane adsorbers comprising grafted glycopolymers for targeted lectin binding
H. C. S. Chenette and S. M. Husson, *J. Appl. Polym. Sci.* 2015, **DOI: 10.1002/app.41437**

Journal of Applied Polymer Science

Hemodialysis membrane surface chemistry as a barrier to lipopolysaccharide transfer

Ben Madsen,[1] David W. Britt,[1] Chih-Hu Ho,[2] Michael Henrie,[2] Cheryl Ford,[2] Eric Stroup,[2] Brent Maltby,[2] Doug Olmstead,[2] Marion Andersen[2]

[1]Biological Engineering Department, Utah State University, Logan, Utah 84322

[2]Dialyzer R&D Department, Fresenius Medical Care North America, Ogden, Utah 84404

Correspondence to: D. W. Britt (E-mail: david.britt@usu.edu)

ABSTRACT: During hemodialysis bacterial lipopolysaccharide (LPS) in contaminated dialysate solution may translocate across the hollow fiber membrane (HFM) to a patient's blood, resulting in fever and possible systemic shock. This study investigates LPS transfer across, and adsorption within, native and modified Fresenius Optiflux® F200NR^{e} polysulfone (PS)/polyvinyl pyrrolidone (PVP) HFMs. Modifications include varied PVP content, addition of a PS-poly(ethylene glycol) copolymer (PS-PEG), and bleach sterilization. Under clinically relevant flow conditions LPS from >400 EU mL^{-1} spiked dialysate is not detected (<0.1 EU mL^{-1}) in the lumens of native fibers, but is detected to varying degrees (0.2–15 EU mL^{-1}) in the lumens of the modified fibers. Fluorescently labeled LPS predominantly adsorbs near the lumen of all membranes except the PS-PEG containing membrane, where LPS localizes on the outer wall. Thus, addition of PS-PEG may entrap LPS in the HFM spongy matrix, away from the blood-contacting fiber lumen. © 2014 Wiley Periodicals, Inc. J. Appl. Polym. Sci. **2015**, *132*, 41550.

KEYWORDS: applications; biomedical applications; fibers; membranes

Received 30 July 2014; accepted 25 September 2014

DOI: 10.1002/app.41550

INTRODUCTION

Hollow fiber membranes (HFM) are used in hemodialysis to clear the blood of uremic toxins that accumulate to dangerous levels in patients with end stage renal failure. Blood is passed through the fiber lumen while dialysate is circulated in a tangential flow outside of the fiber bundles. As blood toxins diffuse into the dialysate it is also possible for any impurities in the dialysate to enter the blood through back-filtration—this is of particular concern for dialysate contaminated with bacterial endotoxin, or lipopolysaccharide (LPS).[1–7] Use of high-flux dialyzers, which remove large percentages of middle molecular weight toxins such as β_2-microglobulin (MW 11 kDa), further raises the potential of back-filtration of LPS in contaminated dialysate.[5,8,9]

LPS is a surface-recognition constituent of gram-negative bacterial membranes consisting of three main parts: an outer-membrane-integrated lipid (lipid A), a core oligosaccharide, and a long heteropolysaccharide chain (O-antigen).[10] The O-antigen varies among different bacterial strains and is the recognition site for blood-borne antibodies. The lipid A portion is generally conserved among bacterial types and is responsible for inducing cytokine activation and pyrogenic reactions. LPS is an amphiphilic molecule that has been shown to preferentially adsorb to hydrophobic surfaces.[2] In solution LPS varies from monomers of 10 kDa, to micelles of 1000 kDa or larger.[10–12]

Bacterial contamination in dialysate fluids and clinical water sources is well-documented,[13–16] with diverse communities of culturable bacteria presenting in dialysate fluids, of which *Pseudomonas* is most common.[17–20] Bacteria colonizing surfaces as robust biofilms may present a persistent source of contamination in dialysate water production lines as they are difficult to detect and remove.[14–16] Several studies on water and dialysate quality in clinics throughout the world, in both developed and developing countries, have shown that as many as 20% of the samples tested were above the limit of the recommended standards.[9,18,21–24] Clinical contamination has also been reported to contain fungus, yeast, mycobacteria, and hazardous chemicals.[23–26]

While small quantities of contamination may not always elicit a pyrogenic response, continued exposure to contaminated dialysate is of great concern because a typical patient on hemodialysis therapy will be exposed to 18,000–30,000 L of water annually.[17,27] Reported pyrogenic reactions up to 0.7 per 1000 treatments have been reported, due mainly to pretreatment problems with dialysis water.[17,28,29] Moreover, trace contamination in the dialysis line water can be amplified as dialysate

buffers, such as bicarbonate, provide an ideal environment for bacterial growth.[28]

Removal of LPS from solution is generally achieved using affinity sorbents and filtration. Plasma exchange and charcoal hemoperfusion as well as immobilization to polymyxin B, ceramic membranes, and functionalized nanoparticles have been investigated with varying degrees of success.[8,9,11,30,31] Other chemistries exhibiting a high affinity for LPS include poly-L-lysine, diethylaminoethane, histamine, and histidine,[32] where the cationic polyelectrolytes presumably bind to the negatively charged phosphate groups on LPS.

As the dialysis membrane represents the final barrier between dialysis fluid and the patient, it becomes important to tune physicochemical properties of dialysis membranes to restrict back filtration of LPS to the blood side of the membrane. Several materials and membrane chemical compositions have been studied for their ability to limit LPS back filtration either in preultrafiltration stages or directly during dialysis treatment. Among these are: polysulfone (PS), polyamide, cellulosic triacetate, ceramic, and polyester.[3,7,13,33–38] Reduced back-filtration has been ascribed primarily to LPS adsorption, with filtration also playing a significant role.[1,3] However, it has also been shown that membranes exhibiting similar characteristics prevent back-filtration of LPS to different degrees, indicating that specific membrane physiochemical properties remain to be identified in order to define the key parameters governing transmembrane LPS flux.[2,3,27] Additionally, as modifications of fiber physiochemical properties are explored to improve blood compatibility they may unintentionally influence back-filtration, thus it is desirable to have a fundamental understanding of how fiber physiochemical properties influence LPS transport and sorption.

The present study explores how different chemical and structural modifications to polysulfone/polyvinyl pyrrolidone (PVP) hollow fiber membranes influence LPS distribution within and back-filtration across the membranes challenged with LPS from cultured sources and fluorescently labeled conjugates. To simulate clinical conditions both convective and diffusive experimental configurations were employed as previously described.[3] Modifications included varied PVP content, addition of a PS-poly(ethylene glycol) copolymer (PS-PEG), and bleach sterilization. LPS is detected to varying degrees in the lumens of the modified fibers, but not the native PS/PVP. Fluorescently labeled LPS predominantly adsorbs near the lumen of all membranes except the PS-PEG containing membrane, where LPS localizes on the outer wall. Water contact angle analysis and scanning electron microscopy correlate these trends with altered membrane hydrophobicity and morphology accompanying the modifications.

MATERIALS AND METHODS

Membranes

All experimental fibers were produced using the phase-inversion solution precipitation method[39] with the same spinning parameters (spinneret size, air gap, bore fluid, rinsing time). Fresenius Optiflux® F200NR^e membranes (Fresenius Medical Care North America), PS-PVP membranes sterilized via electron-beam irradiation, were used as the control against which experimental fiber membranes produced on a pilot line (FMCNA, Ogden, UT) were compared. Three experimental fibers were produced using PS as the base polymer with PVP as an additive or a proprietary PS-PEG copolymer. These are referred to as: high-PVP, low-PVP, and copolymer. "high" and "low" PVP content is with respect to that in the commercial Optiflux membranes—where PVP is present between 1 and 10% by weight.[40] The altered PVP concentrations investigated here are maintained within this range. Bleach-treated Optiflux fibers were prepared through exposure to 0.57% effective sodium hypochlorite content from the dialysate side at 70°C for 2 min in order to limit possible membrane damage during sterilization.[41–43] Importantly, pore size change as measured by sieving coefficient was negligible among the modified membranes (data not shown).

Dialysate with Bacterial Culture Filtrates

The contaminated dialysate challenge solution was prepared by inoculating two solutions of trypticase soy broth (TSB) media with *Stenotrophomonas maltophilia* ATCC 13637 and *Pseudomonas aeruginosa* ATCC 27853, respectively. Following 48 h of incubation, cultures were ultrasonicated (2 min at room temperature) and successively filtered using decreasing pore size, down to 0.22 μm. This filtration process maximized LPS fraction with no noticeable activity aberrations during the testing period. The remaining bacterial culture filtrates were then combined, rendering a challenge solution with LPS from both organisms. From this concentrated stock, bicarbonate dialysate was spiked to obtain LPS concentrations between 200 and 500 EU mL^{-1} in the dialysate and stored at 4°C until use.

In Vitro Dialysis Circuit

A model of *in vitro* dialysis previously described was modified for this study (Figure 1).[7,27] Standard dialysis cassettes for clinical use were used for the *in vitro* studies ($n = 3$). Pumps connected to the blood compartment (BC) and dialysate compartment (DC) were first calibrated using sterile saline. Standard dialysis tubing sets (Medisystems) were sterilized and assembled prior to running the dialysis simulation according to the experimental setup in Figure 1. Both the BC and DC were then rinsed with pyrogen-free saline for 15 min to remove any residual endotoxin. Following the saline rinse the simulation commenced by closing the BC circuit (closed loop) and introducing the dialysate challenge solution to the DC circuit (420 ± 24 EU mL^{-1}). The flow through the BC circuit was held constant at 200 mL min^{-1} using a reservoir of approximately 140 mL, while flow through the DC circuit was 500 mL min^{-1}. After 60 min the BC return line was placed in the dialysate challenge reservoir and the inlet blocked, forming a convective circuit as shown in Figure 1. The flow from the BC was lowered to 37 mL min^{-1} and the simulation was run for an additional 60 min, followed by a saline rinse.

Samples of 10 mL were collected from both the BC and DC following the priming saline rinse, and at time 0, 7, 15, 60, 67, 75, and 120 min during the LPS challenges. LPS concentration in all samples and the original culture filtrate was determined by

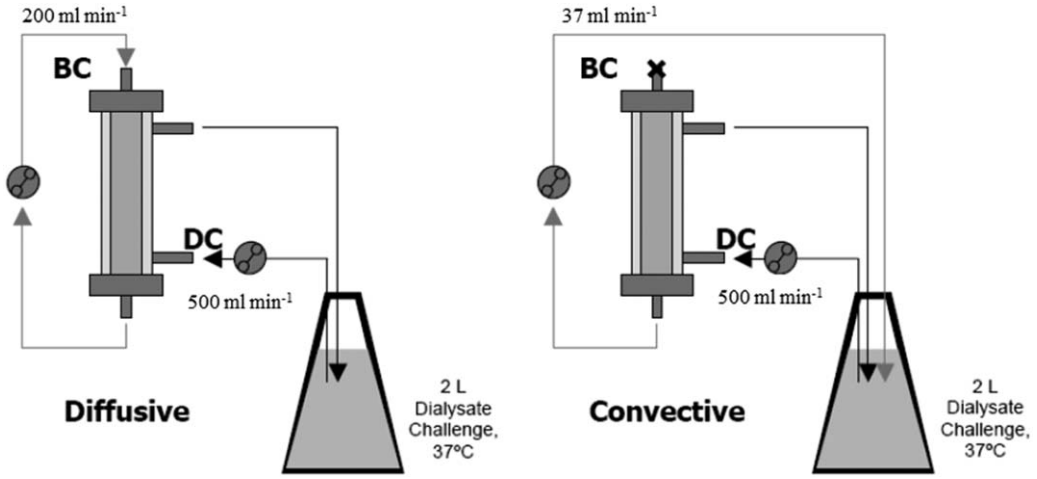

Figure 1. Experimental dialysis simulation setups for the LPS challenge tests. The diffusive setup is first run for 60 min, after which the system is changed to the convective setup and run for an additional 60 min.

kinetic turbidimetric LAL assay (Charles River Labs) having a detection limit of 0.1 EU mL^{-1}.

Fluorescent Imaging

Fluorescence-labeled LPS conjugate (AlexaFluor® 594 conjugate, Invitrogen) was used to localize LPS throughout the membrane wall. Prior studies have shown that a fluorescent label attached to the LPS molecule does not affect the behavior of the LPS.[44] Mini-modules (Figure 2) were constructed for the fluorescent imaging portion of the study to reduce the amount of AlexaFluor® 594 conjugate required. Thirty fibers of each type were placed in a polycarbonate tube (15 cm in length, 2.4 mm inside diameter) and potted using UV-curable epoxy resin (Dymax Corp.). Mini-modules were subjected to the same experimental simulation setup as the full-sized clinical cassettes, with 60 min of diffusive and 60 min of convective testing. Each mini-module was subjected to a challenge of 800 EU mL^{-1} of labeled LPS conjugate in a dark environment. Flow rates for the mini-modules were 1 mL min^{-1} for the BC, 2 mL min^{-1} for the DC.

After the simulations were complete, mini-modules were dried overnight in a vacuum oven at 60°C to prepare for sectioning and imaging. The drying process did not appear to affect fluorophore stability given the strong fluorescence in the obtained images. The process of embedding, slicing, and imaging the samples used a previously described protocol modified for this study.[1,45] Fiber membranes were removed from their housings and sectioned to 10 μm using tissue freezing media (Triangle Biomedical Sciences), a low-profile microtome blade (SEC 35e, Richard-Allan Scientific) and a cryostat (Leica 1850, Leica Microsystems). Sectioned fibers were imaged using a fluorescence microscope (Nikon TE2000-S, Nikon Corp.) with a Resorufin filter set (Chroma Technology). This filter set was used to minimize membrane autofluorescence and maximize fluorescence of the AlexaFluor® 594 conjugate. Images of the membrane samples were obtained with a 12-megapixel camera (Nikon DXM1200, Nikon Corp.) at a resolution of 1280 × 1024 using a 60-s image integration time and analyzed with ACT-1 software (Nikon Corp.). Fluorescence intensity profiles through the fiber cross sections ($n \geq 3$) were measured using ImageJ software (National Institutes of Health).

Figure 2. Mini-module used for fluorescence imaging, showing polycarbonate housing and *Ts*, with UV curable epoxy for potting material. Approximately 30 fibers, 15 cm in length, provide the mini-module with about 15 cm^2 of surface area. [Color figure can be viewed in the online issue, which is available at wileyonlinelibrary.com.]

Surface Characterization by Water Contact Angle

For all membranes tested, sessile drop contact angle analysis was performed on both the outer surface and lumen of the fibers using the method previously described.[43] To access the lumen, the fiber was cut longitudinally and spread open on to double-sided tape. A goniometer (VCA Optima, AST Products) was used to image 0.25 μL droplets of double-distilled water on the surface. Immediately following the application of the droplet, a digital image was captured; from this image the contact angle of the droplet was determined ($n = 8$).

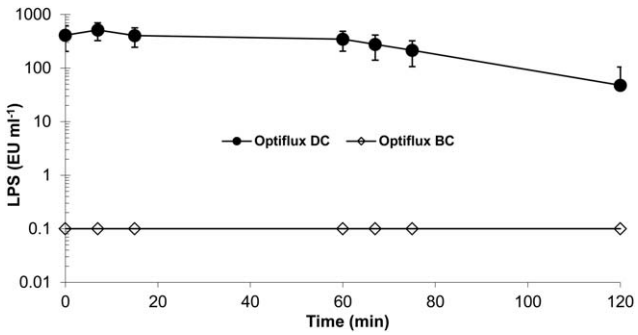

Figure 3. Semilog plot of LPS concentrations in the DC (closed circle) and BC (open circle) for Optiflux (control) membrane (mean ± SD, $n = 3$).

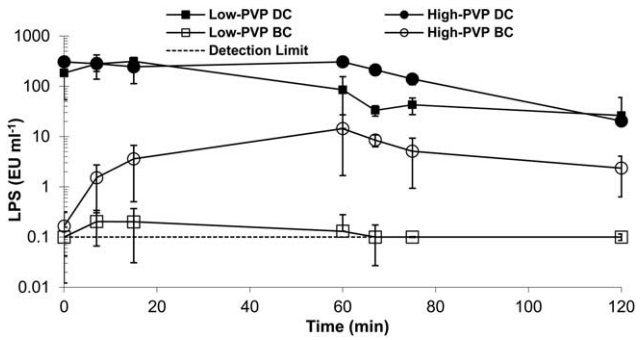

Figure 4. Semilog plot of LPS concentration in BC and DC of high-PVP and low-PVP membranes (mean ± SD, $n = 3$).

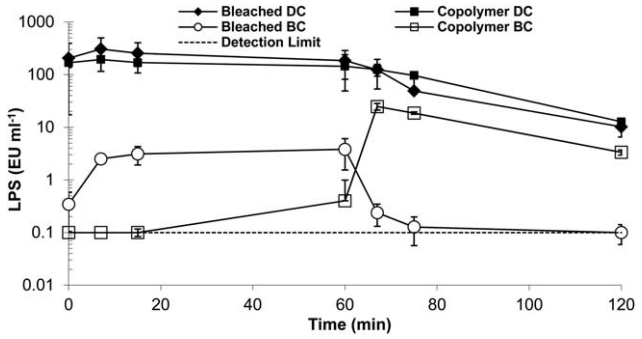

Figure 5. Semilog plot of LPS concentration in BC and DC of bleached and PS-PEG copolymer membranes (mean ± SD, $n = 3$).

SEM Imaging

Fiber membranes were prepared for SEM by dipping the fibers in liquid nitrogen and snapping them with a quick motion, yielding a 90° break. Membranes were then placed onto an imaging stage and coated with gold to 20 nm thick using a sputter coater (Lesker 108, Kurt J. Lesker Co.) and a thickness monitor (Cressington MTM10, Cressington Scientific Instruments). Membranes were then imaged using a field emission scanning electron microscope (Hitachi F-4000, Hitachi).

RESULTS

Dialysis Simulations Using Bacterial Culture Filtrates as Challenge Material

Dialysis simulation data for all membranes tested are shown in Figures 3–5, with curves representing LPS levels measured from the blood compartment and dialysate compartment. Maximum LPS levels in the DC typically occurred from minute 7–15, attributed to the time required for the LPS to equilibrate throughout the system. The decrease in free LPS in the DC with time is attributed to adsorption to the membranes.

Initial LPS levels in the dialysate reservoirs measured by the LAL assay were as follows: Optiflux, 455 ± 44 EU mL^{-1}; low-PVP, 446 ± 73 EU mL^{-1}; high-PVP, 410 ± 107 EU mL^{-1}; bleach, 467 ± 224 EU mL^{-1}; copolymer, 241 ± 43 EU mL^{-1}. During the dialysis simulations LPS was not detected in the BC samples from the Optiflux membrane (Figure 3), indicating any LPS back-filtrate was below 0.1 EU mL^{-1}. In contrast, LPS was detected to varying degrees in the BC in all of the modified membranes following the initial LPS challenge (Figures 4 and 5). Maximum LPS BC concentrations occurred during diffusive conditions for the low-PVP, high-PVP, and bleach treated membranes, whereas LPS concentrations were highest during convective flow for the copolymer fibers. BC peak LPS concentrations were as follows: low-PVP, 0.2 EU mL^{-1} at 7 min.; high-PVP, 14.4 EU mL^{-1} at 60 min.; bleached, 3.8 EU mL^{-1} at 60 min.; copolymer, 24.8 EU mL^{-1} at 67 min.

Surface Hydrophobicity by Contact Angle Analysis

Contact angle measurements were performed on both the outer surface and lumen of the fiber membranes and presented in Figure 6 with mean ± standard deviation for eight samples. The copolymer and high-PVP membranes exhibited significant differences between the outer and lumen contact angles ($P < 0.05$). All lumen contact angles were significantly different from each other, while all outside contact angles were significantly different except Optiflux and high-PVP membranes. Differences in contact angle arise from physicochemical differences among fibers, namely surface roughness, porosity, and concentration and location of the hydrophilic polymer additives, PVP and PEG.

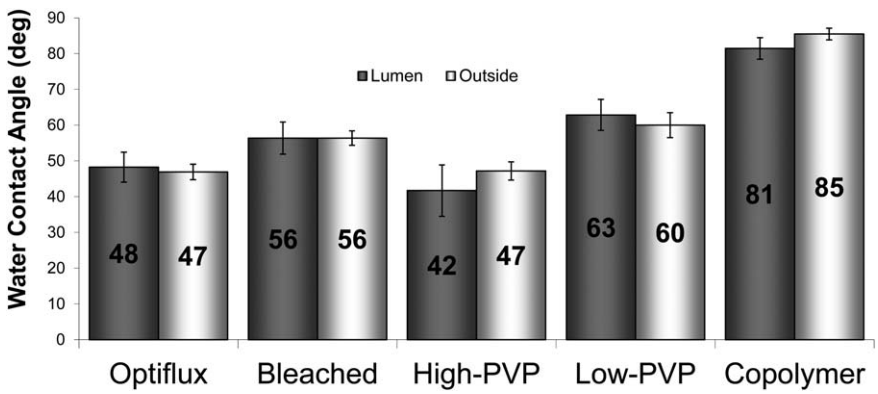

Figure 6. Contact angle measurements of both inner lumen and outside of fiber membranes (mean ± SD, $n = 8$). Statistical analysis revealed significant difference ($P < 0.05$) among all samples. Significant difference between the outside and lumen side contact angle was found only in the copolymer and high-PVP membranes.

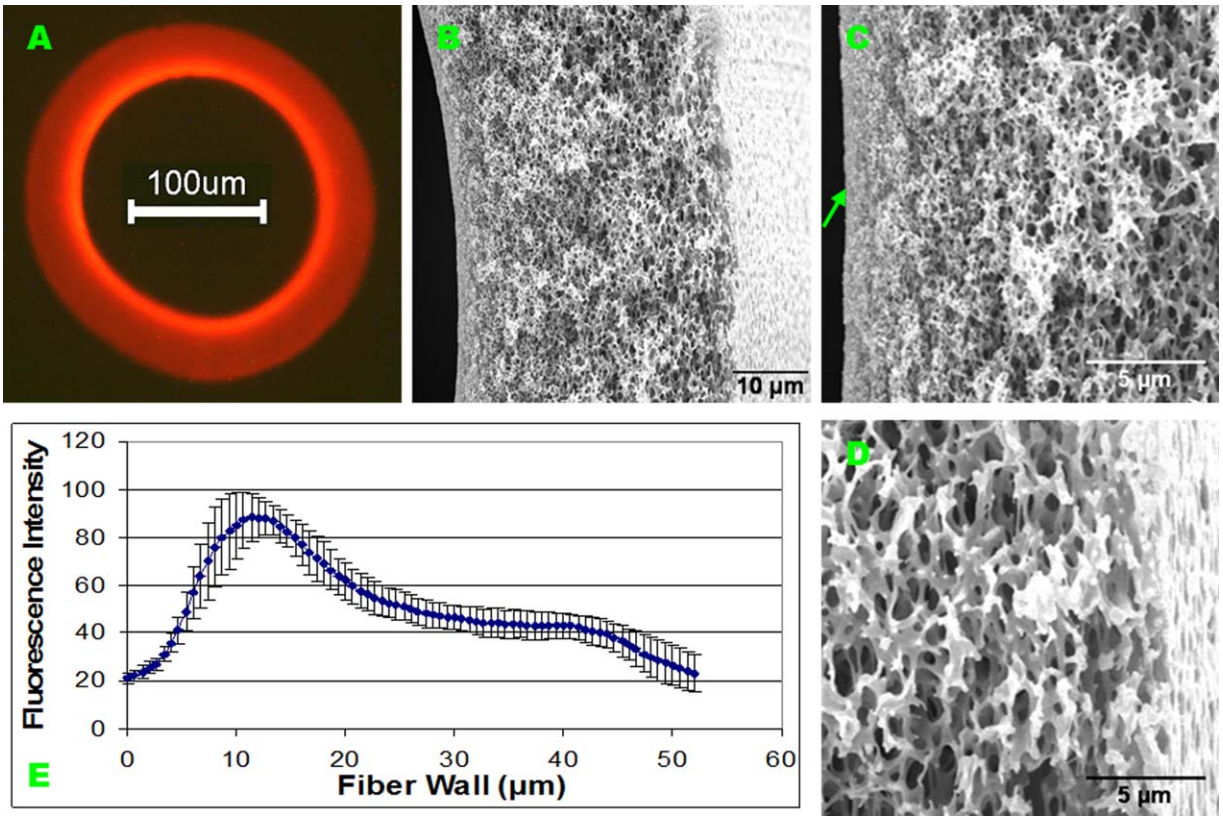

Figure 7. Optiflux membrane: fluorescence image (A), SEM images of the cross section (B), near the lumen (C), and near the outer wall (D), and fluorescence intensity profile (E). Fluorescent-labeled LPS conjugate is distributed throughout the entire membrane cross section, accumulating near the inner lumen surface. The intensity profile shows the distribution of LPS adsorption from lumen (left) to outside (right). The arrow in Panel C indicates the boundary of the lumen wall. [Color figure can be viewed in the online issue, which is available at wileyonlinelibrary.com.]

Imaging of Dialysis Membranes

Fluorescence and SEM images for all membranes tested are presented in Figures 7–11. Differences in the LPS distribution and membrane morphologies can be observed. The arrow in Panel C of Figures 7–11 indicates the boundary of the lumen wall. As seen in the fluorescence images and associated intensity profiles, AlexaFluor-LPS aggregates near the lumen for all fibers except the PS-PEG copolymer, where the opposite was observed. The low-PVP membrane exhibited a higher LPS affinity as indicated by overall image intensity and a more uniform distribution of LPS throughout the fiber spongy matrix as compared to the other fibers. The presented images are representative of all imaged samples ($n \geq 3$ for each fiber type); no atypical fluorescent patterns were observed.

The cross sectional SEM images in Figures 7–11 show similar spongy asymmetric matrix structures for the Optiflux, bleached, high-PVP, and low-PVP membranes. For these membranes the lumen exhibited a less porous wall while the outside structure was a highly porous polymer network. The PS-PEG copolymer membrane (Figure 11) exhibited a "three-layer" structure with a spongy matrix in the outer half of the membrane, a macroporous structure in the inner half, and a compact and continuous structure forming the lumen. Figure 11 reveals macropores extending to the inner wall of the membrane as well as a less porous exterior wall. A clear demarcation in the transition from macropores to spongy matrix is seen in Figure 11(B). The difference in the structure of this membrane can be attributed to distinct thermodynamics of the phase inversion arising from the presence of the PS-PEG block copolymer as compared to PS/PVP fibers, where PVP is the only hydrophilic polymer present.

DISCUSSION

In this study, high concentrations of LPS (roughly 20 times the allowable amount for medical devices) were used to show the ability of hollow fiber membranes to adsorb and filter LPS from solution and to represent a "worst case scenario". However, because experiments were performed at concentrations below the critical aggregation concentration of LPS, similar trends in LPS back-filtration and adsorption would be expected to exist at lower concentrations.[46,47]

Results from the high- and low-PVP simulations (Figure 4) show increases in LPS back-filtration compared to the Optiflux (control) membrane, especially under diffusive conditions. The low-PVP membrane also adsorbed more LPS through the diffusive portion of the simulation, as observed by the sharp decrease in LPS concentration in the dialysate compartment and high intensity in the corresponding fluorescence image. This may correlate to the increased hydrophobicity of this fiber (Figure 6) as discussed later. It is noted that the LPS levels in

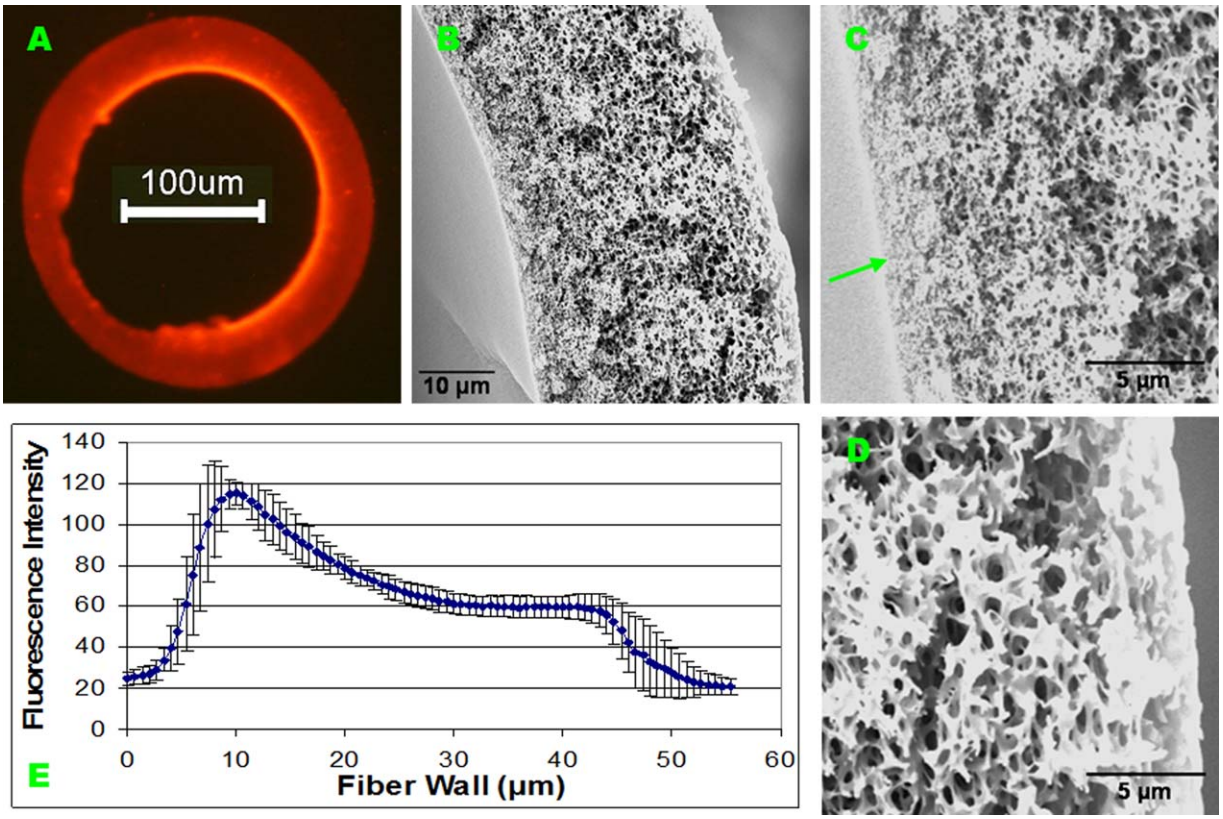

Figure 8. Bleached fiber membrane: fluorescence image (A), SEM images of the cross section (B), near the lumen (C), and near the outer wall (D), and fluorescence intensity profile (E). Fluorescence distribution and surface structure were similar to the Optiflux membrane. The different structure in the bottom left of the fluorescence image is due to cryostat cutting artifact. [Color figure can be viewed in the online issue, which is available at wileyonlinelibrary.com.]

the blood compartment decreased with time during diffusive conditions and immediately dropped below the detection limit during convective conditions for the low-PVP membrane. This decrease in BC LPS levels during diffusive conditions suggests that LPS in the BC may have adsorbed to the membrane or reentered the dialysis circuit solution. During convective flow LPS is likely to be adsorbed or forced into fiber pores. The high-PVP membrane allowed the most LPS transfer into the BC compared to all other membranes, possibly due to a greater pore-size in the lumens of these fibers arising from the additional PVP present during the phase-inversion process. SEM images show a thicker wall structure for the high-PVP membrane (46 μm) than all others ($<$38 μm); however, the pores in the fiber lumens could not be resolved.

It has been shown previously that dialyzers reprocessed using Renalin® (a sterilant composed of hydrogen peroxide, peracetic acid, acetic acid, and water) resisted trans-membrane passage of LPS during treatments.[48] Similarly, polysulfone dialyzers subjected to 13 volumes of a bleach solution were able to effectively remove endotoxin from a challenge solution.[49] In contrast, bleached membranes in this study allowed LPS back-diffusion immediately upon commencement of the diffusive simulation, but less under convective conditions. This highlights how solute transport characteristics are greatly dependent on both the membrane properties and the reprocessing (sterilization) technique.[42,50] Extended bleach sterilization renders PS/PVP fibers increasingly hydrophobic,[43] which may favor LPS binding.

Fiber hydrophobicity is also a key parameter in determining hemocompatibility, which in turn dictates how much anticoagulant must be administered to the patient during dialysis. Reduced administration of heparin or other anticoagulants is desirable, and thus surface modifying layers such as PEG are often explored for blood contacting polymers. Under controlled conditions PEG immobilized on surfaces presents a protein-repellant layer.[51] PS-PEG copolymers have previously been incorporated into PS filter membranes to repel proteins and to enhance surface wettability.[52,53] Here it is observed that the PS-PEG copolymer incorporated in the fibers during the phase-inversion process had unanticipated effects on fiber morphology and LPS distribution. The fluorescence, SEM, and contact angle data indicate that incorporation of PS-PEG into the spin mass resulted in a unique three-layer fiber structure. This fiber readily bound LPS while restricting adsorption to the outermost region of the membrane. Back-filtration of LPS, however, was observed after 7 min of the diffusive simulation. Under convective conditions the membrane allowed a greater passage of LPS to the BC, while also adsorbing most of the LPS in the challenge solution as noted by the decrease in DC LPS concentration. It is observed that the LPS concentration in the BC remained at or near the detection limit for most of the diffusive conditions for

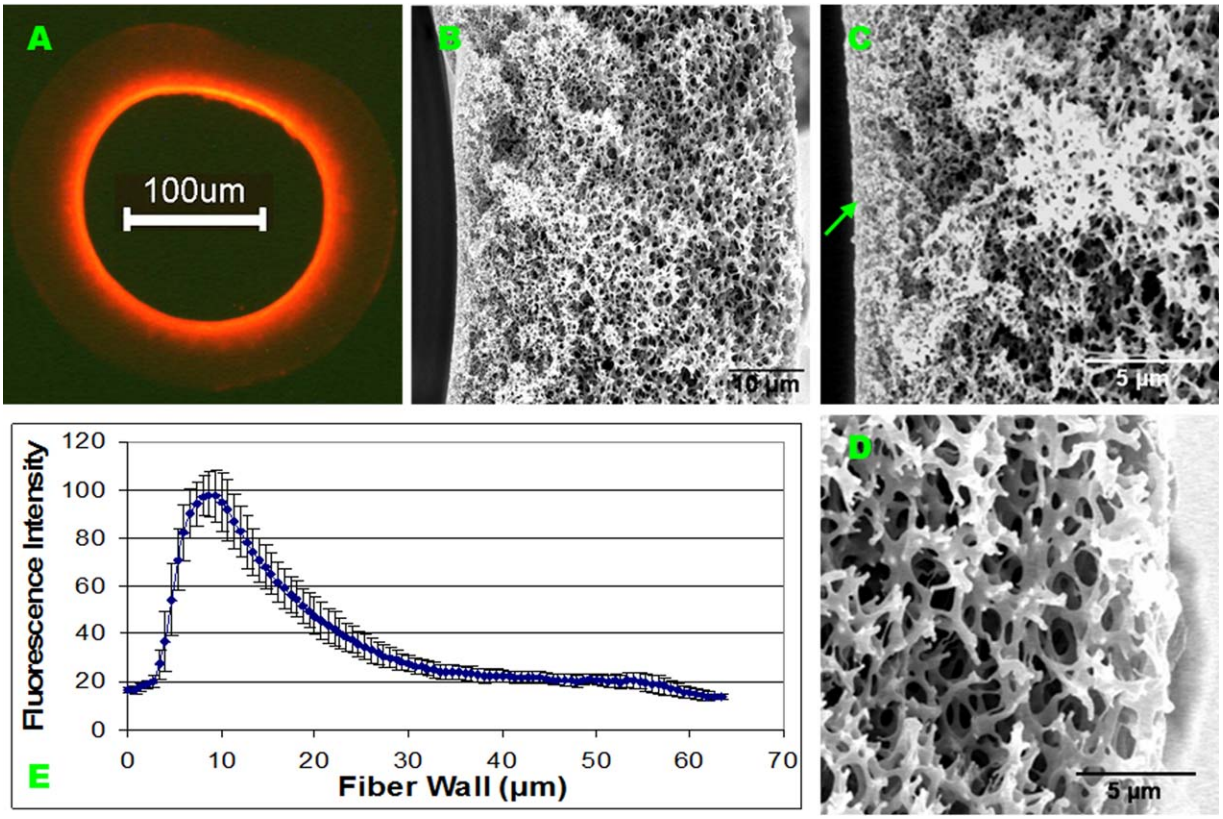

Figure 9. High-PVP membrane: fluorescence image (A), SEM images of the cross section (B), near the lumen (C), and near the outer wall (D), and fluorescence intensity profile (E). Fluorescence intensity for the matrix portion of the membrane is much lower for this sample compared to the other samples indicating less adsorption of LPS. [Color figure can be viewed in the online issue, which is available at wileyonlinelibrary.com.]

the PS-PEG copolymer membrane, and then increased to about 0.4 EU mL^{-1} by 60 min. In contrast to the other membranes, the BC LPS concentration increased upon switching to convective conditions for the copolymer fiber. It is also seen in the SEM cross section that the spongy matrix pores in the copolymer fiber are much smaller near the outer wall, which may restrict the transport of LPS into the BC during diffusive conditions. The PS-PEG copolymer thus renders a fiber with strong LPS binding characteristics away from the fiber lumen, but the process needs to be optimized to avoid the associated increase in LPS flux into the BC under convective conditions.

To address the distribution of PVP and PEG we employed water contact angle analysis of fiber lumens and outside walls (Figure 6). PVP, a common additive to PS membranes, is used to decrease hydrophobicity, increase biocompatibility, and create pores during the phase inversion process.[54] The water contact angles for lumen and outer wall for the Optiflux membrane were 48 and 47, respectively, similar to values previously reported.[3] Increasing or reducing PVP concentration is reflected in the lower and higher contact angles for the high- and low-PVP membranes, respectively, compared to the Optiflux standard. Bleaching of PS-PVP membranes has been shown to cause an increase in hydrophobicity and net negative charge,[43] attributed to chain scission of PVP via radical reactions.[50,55–57] This appears to be occurring here as bleaching Optiflux fibers for 2 min increased fiber hydrophobicity.

Unlike PVP, the PS-PEG additive is an amphiphilic copolymer, which will influence phase separation during the fiber precipitation process as suggested by the "3-layer" structure observed in the SEM cross section. The higher contact angles observed for the PS-PEG membrane suggest the hydrophobic polysulfone blocks of the PS-PEG copolymer are exposed on these surfaces. It is possible that the PEG chains are sequestered in the fiber matrix while PS is concentrated at the interfaces (outside wall and lumen), thus causing an increase in contact angle of these surfaces, and subsequently less LPS adsorption through the spongy matrix. The increase in outside membrane contact angle is different than a previous study that suggested that PEG chains segregated to the outside surfaces of the membrane resulting in a more hydrophilic surface.[52,53] The phase inversion process is by nature, however, sensitive to small changes in spin-mass composition, which can thus dramatically alter thermodynamic partitioning of the polymers in the spin-mass during precipitation.[39] These results suggest that by tuning the PS:PEG ratio and refining the spinning conditions it may be possible to eliminate LPS entry into the BC while maintaining LPS adsorption to the outer wall.

It has been shown that LPS preferentially binds to hydrophobic membranes and that PVP restricts adsorption of proteins to PS membranes.[54,58] Therefore, it would be expected, based on contact angles, that the bleached, low-PVP, and copolymer membranes would bind more LPS than the Optiflux control. Fluorescence images and intensity profiles show that LPS bound extensively

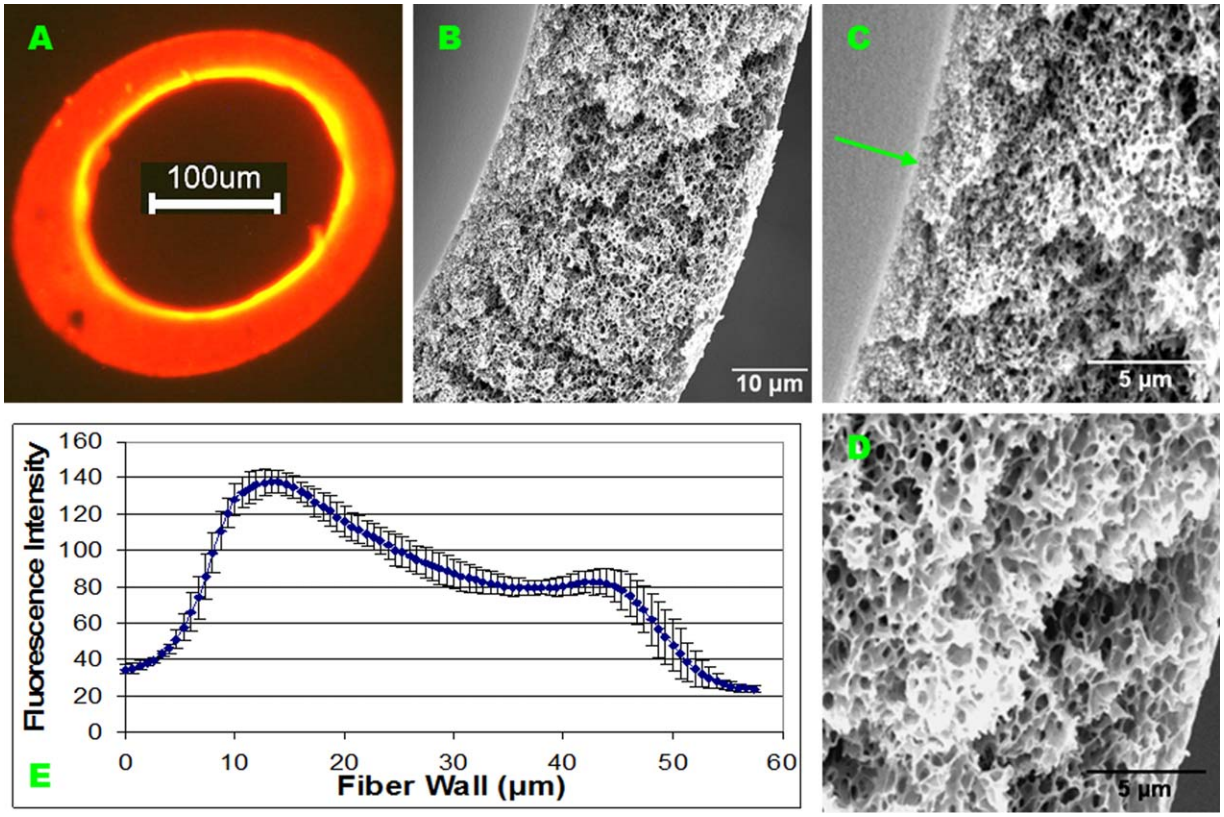

Figure 10. Low-PVP fiber membrane: fluorescence image (A), SEM images of the cross section (B), near the lumen (C), and near the outer wall (D), and fluorescence intensity profile (E). Distribution of LPS for this membrane is similar to the Optiflux membrane; however, intensity is higher indicating a greater affinity of the LPS to this membrane. [Color figure can be viewed in the online issue, which is available at wileyonlinelibrary.com.]

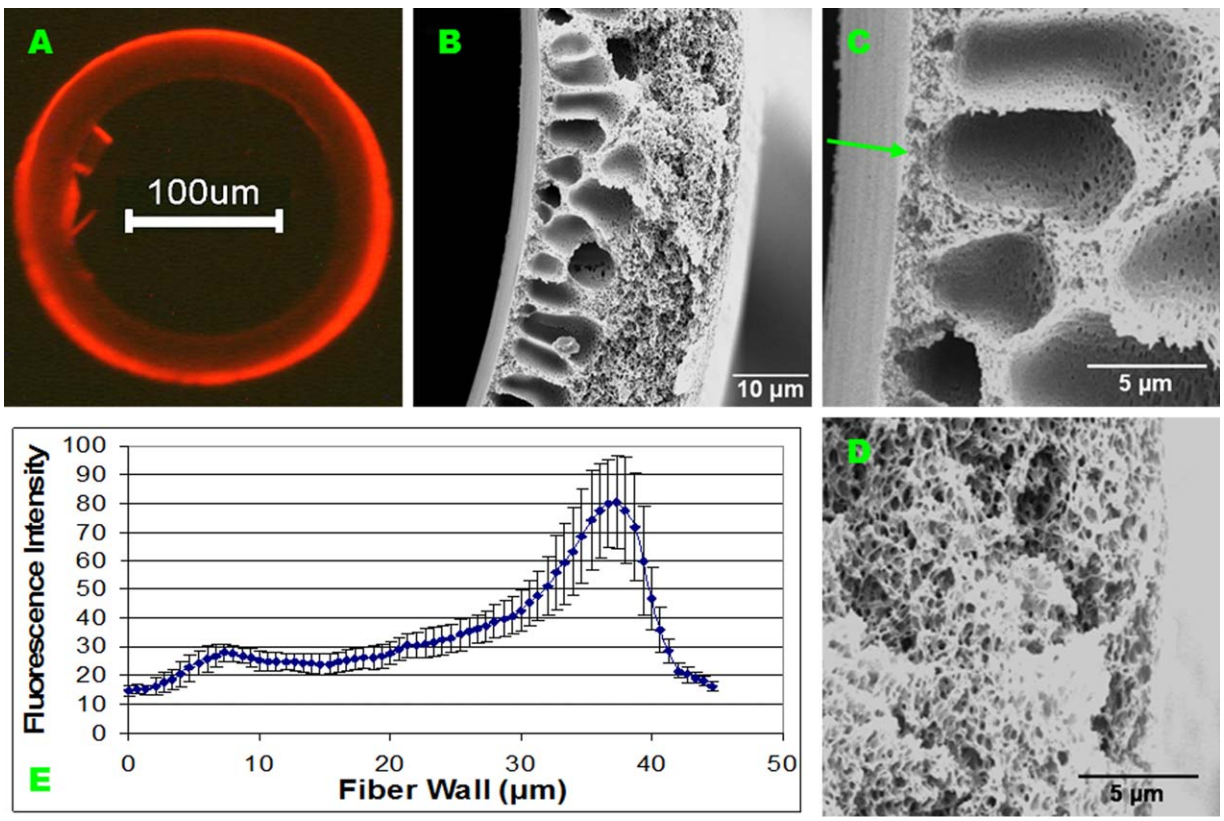

Figure 11. PS-PEG copolymer fiber membrane: fluorescence image (A), SEM images of the cross section (B), near the lumen (C), and near the outer wall (D), and fluorescence intensity profile (E). In contrast to the other fiber types, a distinct transition in the porosity of the spongy matrix is observed and LPS is restricted to the outer surface. [Color figure can be viewed in the online issue, which is available at wileyonlinelibrary.com.]

through the matrix of the low-PVP membrane but only to the outside of the PS-PEG copolymer membrane. LPS also bound more prevalently through the matrix of the bleached membrane compared to the Optiflux membrane, suggesting a chemical makeup in the spongy matrix similar to the low-PVP membrane. PVP content is likely diminished throughout the membrane as indicated by the increase in contact angle compared to the Optiflux membrane. Also, LPS bound only near the lumen of the more hydrophilic high-PVP membrane and not through the matrix of the hollow fiber. SEM images for all membranes except the copolymer show a relatively thick lumen wall. It is likely that LPS in these membranes was trapped near the lumen because of this wall structure. Conversely, the copolymer fiber had much larger macropores near the lumen that may have allowed LPS to more readily reach the BC. Therefore, adsorption of LPS is likely due to both hydrophobic interactions as well as physical entrapment by micropores within the membrane.

In summary, all modified membranes allowed some back-filtration of LPS in the simulation. The average total reduction in LPS from the DC for all membranes tested was ~94% at 120 min, similar to previous studies.[3,59] The distribution of LPS within the membranes suggests that modifications can sequester the bound LPS away from the blood-contacting fiber lumen. Restricting LPS adsorption to the outside wall of the copolymer membrane is viewed as beneficial as it has been shown that LPS does not need to be in direct contact with blood to elicit a pyrogenic response.[12] Although LPS was not detected in the BC of the Optiflux fiber, the possibility of pyrogenic response is still of concern as LPS was observed predominantly near the lumen and may also be crossing the lumen into the BC below the LAL detection limits.

CONCLUSION

The evolution toward high-flux dialysis membranes coupled with bicarbonate dialysate in hemodialysis warrants assessment of pyrogen adsorption to and distribution within the membranes. The data from the experimental fibers investigated here suggest that the physiochemical properties of PS/PVP membranes can be tuned to favor LPS adsorption and possibly prevent back-filtration into the blood compartment of dialyzers. Postprocessing of fibers through bleach sterilization at low concentration and short exposure time led to significant changes in LPS back-filtration and fiber surface properties, demonstrating that simple and commonly used sterilizing (reprocessing) protocols may have unintended consequences on back-filtration. Furthermore, it was shown that the incorporating a PEG block copolymer into the fiber induced changes in membrane porosity, surface chemistry, and LPS adsorption characteristics. Of most significance was the ability of the PS-PEG membrane to adsorb LPS primarily on the outside of the membrane, suggesting a means of sequestering LPS away from the blood-contacting fiber lumen.

REFERENCES

1. Hayama, M.; Miyasaka, T.; Mochizuki, S.; Asahara, H.; Yamamoto, K.; Kohori, F.; Tsujioka, K.; Sakai, K. *J. Membr. Sci.* **2003**, *219*, 15.
2. Takemoto, Y.; Nakatani, T.; Sugimura, K.; Yoshimura, R.; Tsuchida, K. *Artif. Organs* **2003**, *27*, 1134.
3. Henrie, M.; Ford, C.; Andersen, M.; Stroup, E.; Diaz-Buxo, J.; Madsen, B.; Britt, D.; Ho, C.-H. *Artif. Organs* **2008**, *32*, 701.
4. Gong, D.; Ji, D.; Zhang, K.; Huang, X.; Huang, G.; Xu, B.; Liu, Z. *Hemodial. Int.* **2012**, *17*, 618.
5. Schiffl, H. *Semin. Dial.* **2011**, *24*, 1.
6. Canaud, B.; Lertdumrongluk, P. *Nephro-Urol Mon.* **2012**, *4*, 519.
7. Henrie, M.; Ford, C.; Stroup, E.; Ho, C.-H. In Dialysis Membrane Manipulation for Endotoxin Removal. In Progress in Hemodialysis—From Emergent Biotechnology to Clinical Practice, Carpi, A., Donadio, C., Tramonti, G., Eds.; InTech Publishers: Rijeka, Croatia, **2011**.
8. Bender, H.; Pfläzel, A.; Saunders, N.; Czermak, P.; Catapano, G.; Vienken, J. *Artif. Organs* **2000**, *24*, 826.
9. Linnenweber, S.; Lonnemann, G. *ASAIO J.* **2000**, *46*, 444.
10. Gorbet, M. B.; Sefton, M. V. *Biomaterials* **2005**, *26*, 6811.
11. Darkow, R.; Groth, T.; Albrecht, W.; Lützow, K.; Paul, D. *Biomaterials* **1999**, *20*, 1277.
12. Yamamoto, K.; Matsuda, M.; Hayama, M.; Asutagawa, J.; Tanaka, S.; Kohori, F.; Sakai, K. *J. Membr. Sci.* **2006**, *272*, 211.
13. Bambauer, R.; Walther, J.; Jung, W. K. *Blood Purif.* **1990**, *8*, 309.
14. Man, N. K.; Degremont, A.; Darbord, J. C.; Collet, M.; Vaillant, P. *Artif. Organs* **1998**, *22*, 596.
15. Hoenich, N. A.; Levin, R. *Semin. Dial.* **2003**, *16*, 492.
16. Marion-Ferey, K.; Leid, J. G.; Bouvier, G.; Pasmore, M.; Husson, G.; Vilagines, R. *Artif. Organs* **2005**, *29*, 475.
17. ANZSN Consensus Statement for Maintenance of Chemical and Microbiological Safety of Haemodialysis Water and Dialysate Systems; Australian and New Zealand Society of Nephrology: Sydney, Australia, **1996**.
18. Jaber, B. L.; Gonski, J. A.; Cendoroglo, M.; Balakrishnan, V. S.; Razeghi, P.; Dinarello, C. A.; Pereira, B. *J. Blood Purif.* **1998**, *16*, 210.
19. Tsuchida, K.; Nakatani, T.; Sugimura, K.; Yoshimura, R.; Matsuyama, M.; Takemoto, Y. *Artif. Organs* **2004**, *28*, 231.
20. Gomila, M.; Gascó, J.; Busquets, A.; Gil, J.; Bernabeu, R.; Buades, J. M.; Lalucat, J. *FEMS Microbiol. Ecol.* **2005**, *52*, 101.
21. Lonnemann, G.; Sereni, L.; Lemke, H. D.; Tetta, C. *Artif. Organs* **2001**, *25*, 951.
22. Braimoh, R. W.; Mabayoje, M. O.; Amira, C. O.; Bello, B. T. *Hemodial. Int.* **2014**, *18*, 148.
23. Coulliette, A. D.; Arduino, M. *J. Semin. Dial.* **2013**, *26*, 427.
24. Glorieux, G.; Neirynck, N.; Veys, N.; Vanholder, R. *Nephrol. Dial. Transplant.* **2012**, *27*, 4010.
25. Schiavano, G. F.; Parlani, L.; Sisti, M.; Sebastianelli, G.; Brandi, G. *J. Hosp. Infect* **2014**, *86*, 194.
26. Figel, I. C.; Marangoni, P. R. D.; Tralamazza, S. M.; Vicente, V. A.; Rocio Dalzoto, P.; Nascimento, M. M. F.; Hoog, G. S.; Pimentel, I. C. *Mycopathologia* **2013**, *175*, 413.

27. Weber, V.; Linsberger, I.; Rossmanith, E.; Weber, C.; Falkenhagen, D. *Artif. Organs* **2004**, *28*, 210.
28. Gordon, S. M.; Oettinger, C. W.; Bland, L. A.; Oliver, J. C.; Arduino, M. J.; Aguero, S. M.; McAllister, S. K.; Favero, M. S.; Jarvis, W. R. *J. Am. Soc. Nephrol.* **1992**, *2*, 1436.
29. Roth, V. R.; Jarvis, W. R. *Semin. Dial.* **2000**, *13*, 92.
30. Tetta, C.; Bellomo, R.; Inguaggiato, P.; Wratten, M. L.; Ronco, C. *Ther. Apher. Off. J. Int. Soc. Apher. Jpn Soc. Apher.* **2002**, *6*, 109.
31. Sato, T.; Shoji, H.; Koga, N. *Ther. Apher. Dial. Off. Peer-Rev. J. Int. Soc. Apher. Jpn Soc. Apher. Jpn Soc. Dial. Ther.* **2003**, *7*, 252.
32. Anspach, F. B.; Hilbeck, O. *J. Chromatogr. A* **1995**, *711*, 81.
33. Oliver, J. C.; Bland, L. A.; Oettinger, C. W.; Arduino, M. J.; Garrard, M.; Pegues, D. A.; McAllister, S.; Moone, T.; Aguero, S.; Favero, M. S. *Artif. Organs* **1992**, *16*, 141.
34. Rietschel, E. T.; Kirikae, T.; Schade, F. U.; Mamat, U.; Schmidt, G.; Loppnow, H.; Ulmer, A. J.; Zähringer, U.; Seydel, U.; Di Padova, F. *FASEB J. Off. Publ. Fed. Am. Soc. Exp. Biol.* **1994**, *8*, 217.
35. Tellingen, A. van; Grooteman, M. P. C.; Pronk, R.; Loon, J. van; Vervloet, M. G.; Wee, P. M. ter; Nubé, M. J. *ASAIO J.* **2002**, *48*, 383.
36. Czermak, P.; Ebrahimi, M.; Catapano, G. *Int. J. Artif. Organs* **2005**, *28*, 694.
37. Kashiwagi, T.; Sato, K.; Kawakami, S.; Kiyomoto, M.; Takei, H.; Suzuki, T.; Genei, H.; Nakata, H.; Iino, Y.; Katayama, Y. *J. Nippon Med. Sch Nippon Ika Daigaku Zasshi* **2011**, *78*, 214.
38. Erley, C. M.; Herrath, D. von; Hartenstein-Koch, K.; Kutschera, D.; Amir-Moazami, B.; Schaefer, K. *ASAIO Trans. Am. Soc. Artif. Intern. Organs* **1988**, *34*, 205.
39. Mulder, J. Basic Principles of Membrane Technology, 2nd ed.; Kluwer Academic Publishers: The Netherlands, **1996**.
40. Heilmann, K. Asymmetrical Microporous Hollow Fiber for Hemodialysis, Patent CA 1294745 C, **1990**.
41. Sundaram, S.; Barrett, T. W.; Meyer, K. B.; Perrella, C.; Neto, M. C.; King, A. J.; Pereira, B. J. *J. Am. Soc. Nephrol. JASN* **1996**, *7*, 2183.
42. Cheung, A. K.; Agodoa, L. Y.; Daugirdas, J. T.; Depner, T. A.; Gotch, F. A.; Greene, T.; Levin, N. W.; Leypoldt, J. K. *J. Am. Soc. Nephrol. JASN* **1999**, *10*, 117.
43. Madsen, B.; Britt, D. W.; Griffiths, F.; McKenna, E.; Ho, C.-H. *J. Appl. Polym. Sci.* **2011**, *119*, 3429.
44. Levels, J. H.; Abraham, P. R.; Ende, A. van den; Deventer, S. J. *van. Infect Immun.* **2001**, *69*, 2821.
45. Hayama, M.; Miyasaka, T.; Mochizuki, S.; Asahara, H.; Tsujioka, K.; Kohori, F.; Sakai, K.; Jinbo, Y.; Yoshida, M. *J. Membr. Sci.* **2002**, *210*, 45.
46. Aurell, C. A.; Wistrom, A. O. *Biochem. Biophys. Res. Commun.* **1998**, *253*, 119.
47. Bergstrand, A.; Svanberg, C.; Langton, M.; Nydén, M. *Colloids Surf. B Biointerfaces* **2006**, *53*, 9.
48. Teehan, G. S.; Guo, D.; Perianayagam, M. C.; Balakrishnan, V. S.; Pereira, B. J. G.; Jaber, B. L. *Blood Purif.* **2004**, *22*, 329.
49. Weber, C.; Groetsch, W.; Schlotter, S.; Mitteregger, R.; Falkenhagen, D. *Artif. Organs* **2000**, *24*, 323.
50. Shao, J.; Wolff, S.; Zydney, A. L. *Artif. Organs* **2007**, *31*, 452.
51. Leckband, D.; Sheth, S.; Halperin, A. *J. Biomater. Sci. Polym. Ed.* **1999**, *10*, 1125.
52. Hancock, L. F.; Fagan, S. M.; Ziolo, M. S. *Biomaterials* **2000**, *21*, 725.
53. Park, J. Y.; Acar, M. H.; Akthakul, A.; Kuhlman, W.; Mayes, A. M. *Biomaterials* **2006**, *27*, 856.
54. Hayama, M.; Yamamoto, K.; Kohori, F.; Sakai, K. *J. Membr. Sci.* **2004**, *234*, 41.
55. Wienk, I. M.; Meuleman, E. E. B.; Borneman, Z.; Boomgaard, T. van den; Smolders, C. A. *J. Polym. Sci. Part Polym. Chem.* **1995**, *33*, 49.
56. Wolff, S. H.; Zydney, A. L. *J. Membr. Sci.* **2004**, *243*, 389.
57. Rouaix, S.; Causserand, C.; Aimar, P. *J. Membr. Sci.* **2006**, *277*, 137.
58. Yamamoto, C.; Kim, S. T. *J. Biomed. Mater. Res.* **1996**, *32*, 467.
59. Nakatani, T.; Tsuchida, K.; Sugimura, K.; Yoshimura, R.; Takemoto, Y. *Int. J. Mol. Med.* **2003**, *11*, 195.